

# Materials Science

An Indian Journal

Full Paper

MSAIJ, 12(8), 2015 [277-283]

## Influence of the silicon content on the high temperature oxidation of a spheroidal graphite cast iron. part 1: Preparation of SG cast iron with various SI contents

Mamadou Saidou Diallo<sup>1,2</sup>, Patrice Berthod<sup>1,2,3\*</sup>

<sup>1</sup>University of Lorraine, (FRANCE)

<sup>2</sup>Faculty of Sciences and Technologies, (FRANCE)

<sup>3</sup>Institut Jean Lamour (UMR 7198), Team 206 "Surface and Interface, Chemical Reactivity of Materials"

B.P. 70239, 54506 Vandoeuvre-lès-Nancy, (FRANCE)

E-mail : patrice.berthod@univ-lorraine.fr

### ABSTRACT

Spheroidal graphite (SG) cast irons sometimes solidify too rapidly to be really constituted of only ferrite and graphite at room temperature. In such cases a heat-treatment of graphitization is compulsory, applying it necessarily induces high temperature oxidation for the pieces surfaces. In not alloyed cast irons the single element possibly limiting this deterioration is silicon. In this study it is wished to start establishing qualitative relationship between the silicon content in a given SG cast iron and the amount of deterioration by hot oxidation provoked by a same thermal cycle. In this first part it was tried to re-melt parts of a same SG cast-iron in order to modify its Si content, but by preserving the spheroidal character of graphite. This was here successfully realized by using a high frequency induction furnace under argon atmosphere for a duration short enough to avoid the fading phenomenon. SG cast iron ingots were thus obtained with different contents in silicon, with graphite particles still spheroidal, but with also a global finer microstructure, notably much higher nodules counts and much smaller nodules. © 2015 Trade Science Inc. - INDIA

### KEYWORDS

Spheroidal graphite  
cast iron;  
Silicon;  
Re-melting;  
Microstructure;  
Hardness.

### INTRODUCTION

Iron-carbon alloys are among the most frequently used metallic alloys since many hundred years<sup>[1,2]</sup>. The low carbon ones, steels<sup>[3]</sup> – which contain typically less than 2wt.% C and furthermore less 1.5wt.% C for most of them – are mechanically very strong at room temperature and also very refractory (melting point of iron: 1535°C<sup>[4]</sup>). These ones may be more or less highly al-

loyed with many other elements and elaborated/treated following a great number of different ways in order to achieve very various mechanical, chemical or physical properties.

The high carbon {Fe, C}-based alloys, cast irons, may be themselves of very numerous types. Their matrix may be ferritic, ferrite-pearlitic, pearlitic, ledeburitic this following the cooling rate during solidification and after down to room temperature, bainitic or martensitic

## Full Paper

if salts-, oil- or water-quenched. If they solidified in the austenite-graphite system rather than in the austenite-cementite one, the graphite particles may be themselves of different morphologies (flake, vermicular or nodular). As in the case of steels, this multiplicity of microstructure leads to very various properties in many fields.

Concerning especially cast irons<sup>[5,6]</sup> the obtained as-cast microstructures are often not suitable for the expected properties and the shaping by foundry/moulding is generally followed by heat-treatment. For example this one aims to the disappearance of the carbides issued from too fast solidification or the ferrite/pearlite rating when one of these constituents is too present. One of the most used type of cast iron is the spheroidal graphite ferritic one and after solidification it happens that some carbides are also present in the microstructure or a too important fraction of pearlite. A re-heating up to high temperature just under the eutectic plateau (to avoid any partial re-melting and thus possible loss of the spheroidal shape of graphite) for a stage of several minutes, generally allows suppressing such carbides (for rather low initial fractions). And the following slow cooling generally allows solid transformation of austenite into ferrite and graphite, with no appearance of pearlite.

Since such post-solidification heat-treatment is generally carried out in plant's air oxidation necessarily takes place with as result a more or less severe deterioration of the pieces' surface. No aluminium and no chromium<sup>[7,8]</sup> being present in the no-alloyed cast irons the resistance to high temperature oxidation depends on silicon only. Indeed this element is necessarily present in such SG cast alloys elaborated from clean new iron coming from blast furnace, to avoid carbide-forming or carbides-stabilizer elements as this may happen when iron comes from cupola.

In this work a spheroidal graphite cast iron already elaborated was enriched in silicon or not and tested in high temperature oxidation. The applied thermal cycle was characterized by { temperature, time }-values typical of the ones which can be used for destabilizing/dissolving the carbides resulting from to a little too fast solidification, and suppress the initial part of pearlite to obtain a matrix wholly ferritic. In this first part, parts of an available piece of a SG cast iron ingot were re-melted with addition of supplementary silicon in order to ob-

tain SG irons with several Si contents. The microstructures and hardness of these new cast iron ingots will be characterized. In the next part<sup>[9]</sup> of this study these new cast irons will be tested in high temperature oxidation.

## EXPERIMENTAL

An ingot of about 5cm × 5cm × 10cm of spheroidal graphite cast iron in the laboratory was available, the microstructure of which is illustrated by optical micrograph in Figure 1. This ingot is made of a SG cast iron containing effectively nodular graphite but also primary cementite and pearlite.

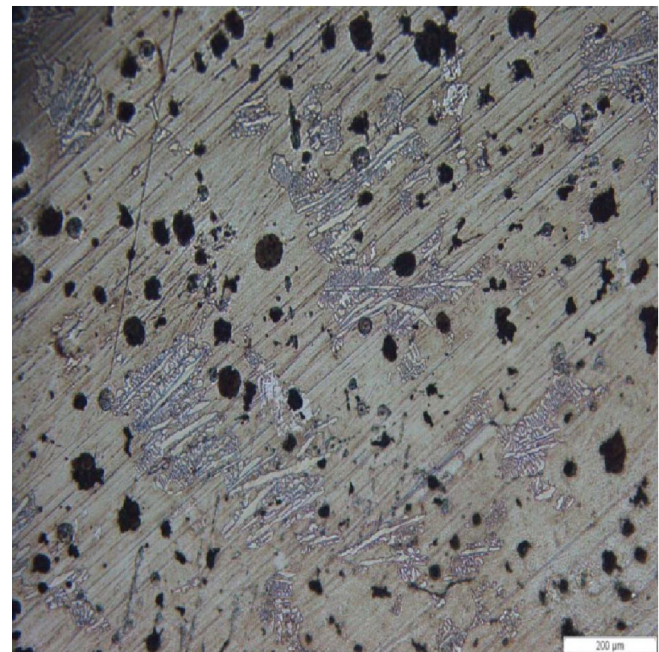


**Figure 1 : Optical micrograph of the microstructure of the initial ingot (after Nital 4 etching)**

Its chemical composition was determined by Energy Dispersion Spectrometry using a Scanning Electron Microscope (SEM) JEOL JSM 6010LA: it is composed of principally iron, carbon (not measurable with this technique) and of 2.53 wt.% of silicon.

This initial ingot was cut to prepare three parts of about 40g to re-melt without or with silicon addition. Cutting, carried out with a Buelher Delta Abrasimet metallographic disc saw, led to three parts weighing 37.33, 39.71 and 38.78g, which were re-melted without silicon addition for the first one (to obtain an ingot with the history then the same microstructure fineness

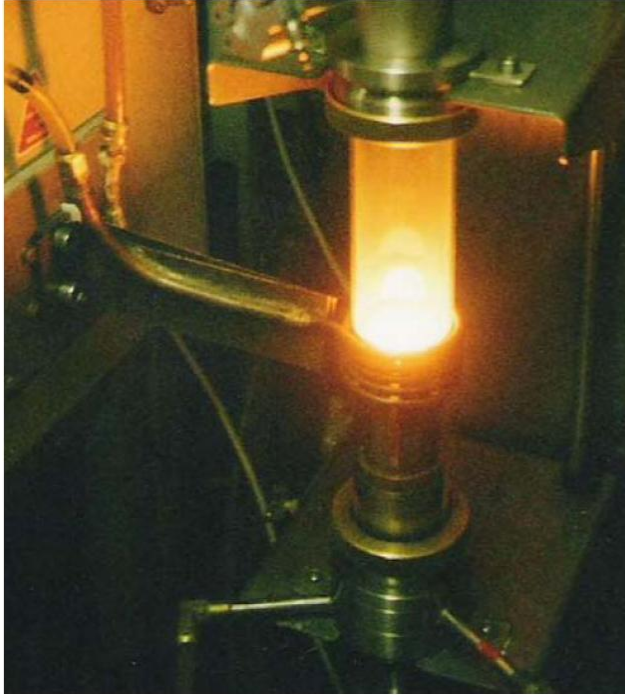


**Figure 2 : Melting in progress in the copper crucible of the high frequency induction furnace**



cycle was applied:

- voltage increased up to 2500 Volts to which it was maintained during one minute.
- new increase in voltage up to 3500 Volts also followed by a 1 minute stage.
- progressive decrease of the applied voltage down to 0 (about 20 seconds of power diminution).

The three ingots were each cut in to halves using a same metallographic disc saw as above. One half was embedded in a cold resin mixture (resin Araldite DBF + hardener HY956, Escil). The mounted sample was ground with SiC-papers from 120 to 1200 grade, under water from 120 up to 800-grit, and without any lubricant for the 1200-grit paper. Indeed grinding in dry condition is compulsory for the final grinding stage to avoid any hydration of the graphite nodules to preserve them from shape deterioration under grinding. After intermediate ultrasonic cleaning the sample was finally polished with textile enriched with 1µm hard particles.

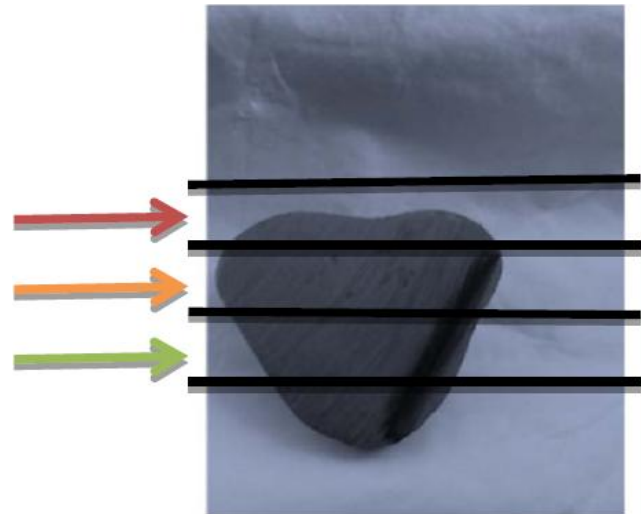


**Figure 3 : General view of the ingot before cutting (left) and areas of metallographic characterization on half ingot (right)**

as the two Si-enriched ingot), with addition of 0.2g of Si for the second one, and with addition of 0.4g Si for the third one. The re-melting was carried out using a CELES high frequency induction 100kW-furnace under an inert atmosphere of pure argon (300 mbars). The photograph given in Figure 2 illustrates the fusion of an alloy in the water-cooled copper crucible of this furnace.

In order to favour the re-appearance of spheroidal graphite in the re-solidified ingots the following thermal

The sample was immersed in a ‘Nital 4’ etchant – composed of 96% ethanol ( $H_3C-CH_2-OH$ ) and 4% pure nitric acid ( $HNO_3$ ) – for about ten seconds to reveal the initial microstructure of this cast iron. Microstructure examinations were performed using a metallographic optical microscope Olympus model BX51 equipped with a digital camera.

Numerical optical micrographs were taken to illustrate microstructure as well as to allow counting of graphite nodules after paper printing and to measure the

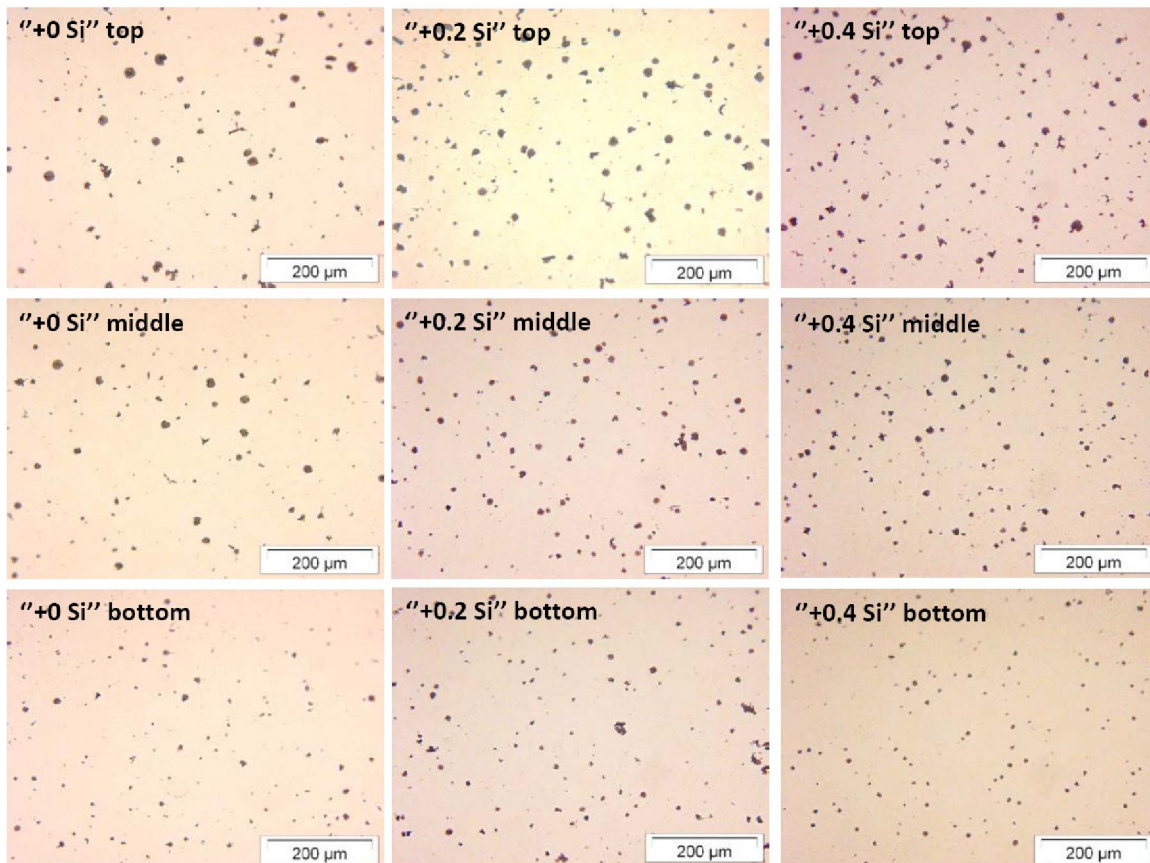


**Figure 4 :** The obtained microstructures of the three re-melted and re-solidified ingots for the three locations (top: red arrow in Figure 4, middle: orange arrow, bottom: green arrow); left: the one without Si addition (2.5 wt.%Si), middle: the one without single Si addition (3.0wt.%Si), right: the one with double Si addition (3.5 wt.%Si)

graphite surface fractions using the image analysis tool of the Adobe Photoshop CS software of Adobe.

Besides, the hardness of the three ingots was specified with Vickers indentations performed on the mounted and polished samples. This was done using a Testwell Wolpert apparatus, with a load of 10kg.

## RESULTS AND DISCUSSION

### Microstructures of the re-melted and re-solidified ingots: qualitative observations

A macrophotograph of one of the obtained ingots is presented in Figure 3, before (left) and after (right) cutting. The arrows (red, orange and green) respectively show the “top”, “middle” and “bottom” localizations in which the microstructures were observed.

Indeed, since the microstructure was often obviously heterogeneous from top to bottom in the ingots it was necessary to do this distinction. The microstructures of the three ingots before Nital etching are pre-

sented by optical micrographs in Figure 4. There are obviously much finer than the one of the initial SG cast iron. This is due to the much faster solidification in the copper crucible of the induction furnace (the solidification of the initial – and bigger – ingot was probably realized in a sand mould). This proves that it was really necessary to re-melt and re-solidify the not Si-enriched cast iron in these new conditions to allow valuable comparisons. It is also very important to notice that the obtained graphite is still of a spheroidal type, despite no additional treatment of liquid metal was done after the re-melting of the initial SG cast iron: neither desulfurization and magnesium treatment, nor inoculation. Second it seems that the graphite nodules are more present or coarser in the upper part of the ingots than bellow, and that their population density is higher for a higher Si content.

### Microstructures of the re-melted and re-solidified ingots: quantitative measurements results

TABLE 1 : surface density and surface fractions of the graphite spheroids (counted/measured on not etched samples)

Final Si content (wt.%)	Localization in the ingot	Nodule count (mm <sup>-2</sup> )	Surface fraction of graphite (surf.%)
Ingot with 2.5% Si (“+0 Si”)	top	51.84 ± 4.13	2.69
	middle	52.60 ± 2.34	2.11
	bottom	51.32 ± 1.59	1.13
Ingot with 3.0% Si (“+0.2 Si”)	top	63.43 ± 7.06	3.55
	middle	55.93 ± 5.13	2.04
	bottom	80.65 ± 24.54	1.81
Ingot with 3.5% Si (“+0.4 Si”)	top	77.07 ± 0.39	3.16
	middle	74.42 ± 4.44	2.17
	bottom	84.32 ± 25.43	2.80

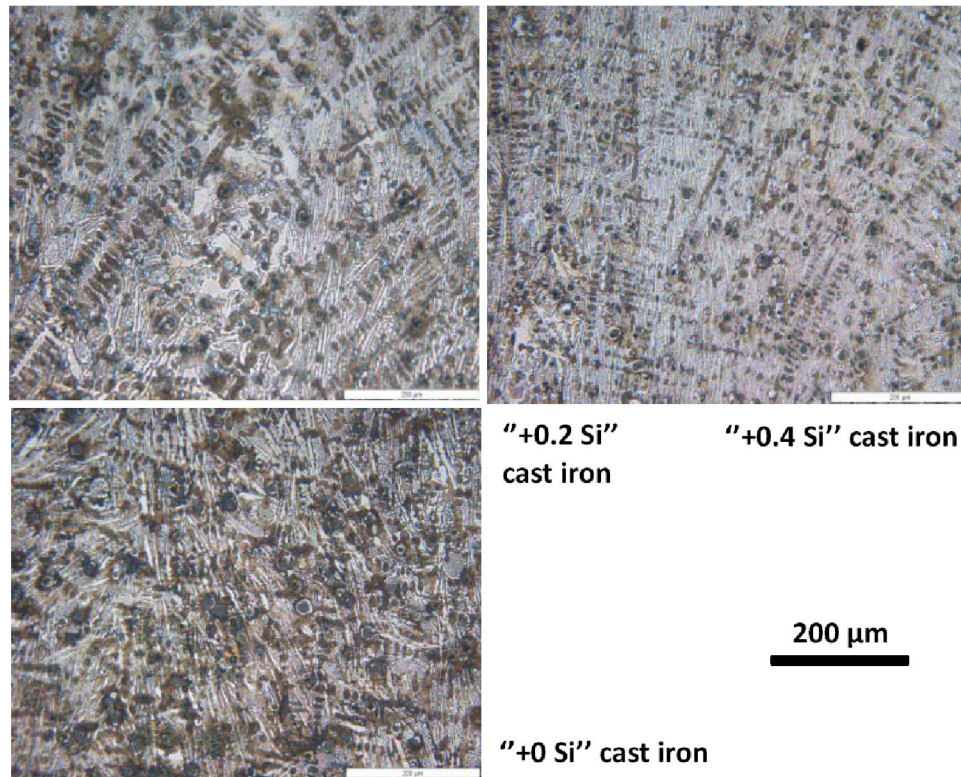


Figure 5 : The global microstructures of the three ingots after Nital etching

In order to get more accurate data about the graphite population, several micrographs were taken in each location, then digitalized in black and white pixels to allow measuring the cumulative surface fractions of graphite. For each ingot and for each location in a same ingot the results led to an average value and a standard deviation one for uncertainty. The results are given in TABLE 1.

From the results presented in this TABLE 1 it appears first that the density of the graphite nodules (as is to say their number of per surface unit area) tends to be higher near the bottom of the ingot than in its highest

part. This difference, which is curiously more visible for the two Si-enriched ingots than for the not Si-enriched one, can be explained by the probably faster solidification of the bottom part of the ingots in contact with the water-cooled metallic crucible, than the upper part which is farther from this crucible. This also explains the presence of coarser nodules in the upper part by comparison with below (Figure 3). Second, for each location – top, middle and bottom – the nodules count gives higher values for higher Si contents. Concerning the surface fractions of graphite it seems that it is systematically higher for the top localization than for the middle

TABLE 2 : Hardness values (Vickers, load: 10kg)

Final Si content (wt.%)	Localisation in the ingot	Hv <sub>10kg</sub>
Ingot with 2.5% Si (“+0 Si”)	top	464
	middle	488
	bottom	525
Ingot with 3.0% Si (“+0.2 Si”)	top	450
	middle	483
	bottom	514
Ingot with 3.5% Si (“+0.4 Si”)	top	401
	middle	478
	bottom	336

one and higher for the middle localization than for the bottom one. In contrast, the variation of the graphite surface fraction with the silicon content is not so clear, but there is however a tendency to an increase when the Si content increases.

### Microstructures of the re-melted and re-solidified ingots: after Nital etching

Etching with the Nital solution generally allows well seeing the microstructure of not alloyed carbon steels and cast irons, pearlite becoming grey while ferrite and cementite remain white. The microstructures of the three ingots after etching are illustrated by optical micrographs in Figure 5. It seems qualitatively that ferrite, cementite and pearlite are respectively slightly more present, less present and less present, when the silicon content increases.

The indentations which were performed according to the Vickers method under a 10kg load led to the values given in TABLE 2. Seemingly the hardness increases from top to bottom in each ingot while, for a given localization, it decreases when the Si content increases. This is in good agreement with the observations made just above about the microstructure evolution since the harder phases or constituent are cementite and pearlite.

### General commentaries

Maybe the most interesting observation that was done here is that spheroidal graphite were obtained after re-melting of the initial SG cast iron and re-solidification. Although that the melting was not achieved with a high power or voltage fusion was probably complete and, besides the initial matrix obviously wholly re-melted, most of the existing graphite nodules have also

disappeared. But, thanks to both the rather low maximal voltage applied and to the short stage in the molten state, the nuclei were still here and furthermore in an active state (no “fading” phenomenon) and they acted during the solidification, leading again to spheroids. Besides, re-melting and stage in the molten stage were realized in inert atmosphere: thus, no oxygen came and promoted any degenerating effect on the growing nodules during solidification. And then: despite the absence of any new desulfurization/spheroidization treatment and of any additional inoculation to help graphite to nucleate notably in this context of competition with cementite because fast solidification, graphite succeeded nucleating and growing as spheroids. The beneficial effects of the desulfurization and inoculation applied for the first solidification of cast iron part were thus still intact.

Thanks to that, it was thus possible to simply obtain in laboratory, with simple re-melting and re-solidification, new ingots of SG cast iron with new levels in silicon contents. But it is true that the faster solidification, rate furthermore depending on the localization in the copper crucible, led to microstructure much finer than initially and heterogeneous matrixes and densities of graphite nodules.

### CONCLUSIONS

New ingots of spheroidal graphite cast irons were then successfully obtained with various silicon contents. The three SG cast irons will be now exploited to explore their responses to high temperature graphitization treatments, in term of behaviour in high temperature oxidation as well as in term of disappearance of carbides (primary cementite and lebeburite during the stage

and pearlite during the cooling through the eutectoid plateau or band). This is the subject of the second part of this work<sup>[9]</sup>.

### ACKNOWLEDGEMENTS

The authors wish to thank Miss Elodie Conrath for her advices which allowed improving this manuscript.

### REFERENCES

- [1] M.Durand-Charre; La Microstructure des aciers et des fontes. Genèse et interprétation, SIRPE, Paris (2003).
- [2] M.Durand-Charre; Microstructure of Steels and Cast Irons – Engineering Materials and Processes, Springer-Verlag, Berlin Heidelberg New York (2004).
- [3] G.Béranger; Le livre de l'acier, Lavoisier, Paris Cachan (1994).
- [4] P.T.B.Shaffer; High-Temperature Materials, Materials Index, Plenum Press, New York (1964).
- [5] J.R.Davis; Cast Irons, ASM International (1996).
- [6] G.Lesoult; Traité des matériaux : Tome 5, Thermodynamique des matériaux : De l'élaboration des matériaux à la genèse des microstructures, Presses Polytechniques et Universitaires Romandes (2010).
- [7] P.Kofstad; High Temperature Corrosion, Elsevier Applied Science (1988).
- [8] D.Young; High Temperature Oxidation and Corrosion of Metals, Elsevier, Amsterdam (2008).
- [9] M.S.Diallo, L.Aranda, P.Berthod; Materials Science: An Indian Journal, to be submitted.